Available online at www.sciencedirect.com

ScienceDirect

www.journals.elsevier.com/journal-of-environmental-sciences

JOURNAL OF ENVIRONMENTAL SCIENCES
www.jesc.ac.cn

Heterogeneous uptake of nitrogen dioxide on Chinese mineral dust

Li Zhou[1,2], *Weigang Wang*[1,*], *Siqi Hou*[1], *Shengrui Tong*[1], *Maofa Ge*[1,*]

1. *Beijing National Laboratory for Molecular Science (BNLMS), State Key Laboratory for Structural Chemistry of Unstable and Stable Species, Institute of Chemistry, Chinese Academy of Sciences, Beijing 100190, China. Email: zhouli@iccas.ac.cn*
2. *Beijing National Laboratory for Molecular Science (BNLMS), State Key Laboratory for Structural Chemistry of Unstable and Stable Species, Peking University, Beijing 100871, China*

ARTICLE INFO

Article history:
Received 19 January 2015
Revised 19 May 2015
Accepted 20 May 2015
Available online 21 July 2015

Keywords:
Mineral dust
Nitrogen dioxide
Uptake coefficient
Temperature dependence

ABSTRACT

Mineral dust is one of the major aerosols in the atmosphere. To assess its impact on trace atmospheric gases, in this work we present a laboratory study of the effect of temperature on the heterogeneous reaction of NO_2 on the surface of ambient Chinese dust over the temperature range from 258 to 313 K. The results suggest that nitrogen dioxide could mainly be adsorbed on these types of Chinese mineral dust reversibly with little temperature dependence. Similar to a previous study on NO_2 uptake on mineral aerosols, the uptake coefficients are mainly on the order of 10^{-6} for the Chinese dust, when BET areas are taken into account. HONO was observed as a product, and its formation and decomposition on Chinese mineral dust during the uptake processes were also studied. The complete dataset from this study was compiled with previous literature determinations. Atmospheric implications of the heterogeneous reaction between NO_2 and mineral dust are also discussed, in an effort to understand this important heterogeneous process.

Introduction

Mineral particulate matter, constituting 36% of total primary aerosol emissions, has been recognized as one of the major aerosols in the troposphere (Ooki and Uematsu, 2005; Sullivan et al., 2007). Annually, about 1000–3000 Tg mineral dust is emitted into the atmosphere (Dentener et al., 1996; Harrison et al., 2001; Usher et al., 2003). Mineral dust can react with various trace gases, and the lifetimes of the various trace gases may change *via* heterogeneous interactions with dust, which can provide reactive sites for surface-mediated heterogeneous reactions (Prospero, 1999; Wagner et al., 2008).

The chemical interactions between mineral dust and pollutants are significant contributors to atmospheric processes; dust plumes that originate from Saharan Africa or central Asia can be transported several thousands of kilometers and mix with air from urban areas (Carmichael et al., 1997; Song and Carmichael, 2001; Tang et al., 2004). As one of the predominant polluting gases, nitrogen dioxide can influence the pH of rainwater and lead to the formation of secondary nitrate aerosols. A typical concentration of NO_2 in the photochemical smog may reach 70 ppb, but in emission sources, such as coal power plant stations and motor engines, the NO_2 concentration may reach as high as 400 ppm (Zamaraev et al., 1994; Lisachenko et al., 2006). With increasing NO_2 concentrations in the troposphere, the importance of NO_2 reactions with mineral dust in the atmosphere needs to be evaluated. From field observation results, it is apparent that mineral dust can affect the local gas-phase concentration of nitrogen dioxide, either by physical adsorption or by heterogeneous reaction. These results have important

* *Corresponding authors.* E-mails: wangwg@iccas.ac.cn (Weigang Wang), gemaofa@iccas.ac.cn (Maofa Ge).

http://dx.doi.org/10.1016/j.jes.2015.05.017

implications for improving the treatment of dust in global chemistry models and highlight a number of key processes that merit further investigation through laboratory and field studies (Guan et al., 2014; Nie et al., 2012; Li et al., 2010; Li and Han, 2010; Sullivan et al., 2007).

Heterogeneous reactions of NO_2 with atmospheric mineral particulates are thought to be a source of atmospheric HONO (Febo et al., 1996). Studies show that high levels of hygroscopic nitrate are generated by the heterogeneous conversion of NO_2 on the surface of particulates in the atmosphere (Al-Abadleh et al., 2003). Heterogeneous processes are thought to be the major source of HONO in the atmosphere. They have been intensively studied in the laboratory, and several mechanisms of HONO formation on aerosols and the ground surface have been proposed (Cwiertny et al., 2008). The enhanced NO_2 conversion could be an important HONO, and therefore also OH, source in regions where pollution and dust storms coincide (Kleffmann, 2007; Wang et al., 2003), while the contribution of mineral aerosol to the HONO loss in the atmosphere is limited (El Zein et al., 2013).

In this study, we investigated the heterogeneous uptake of NO_2 on two different solid particles representative of mineral dust from the Inner Mongolia desert and Xinjiang arid region. The temperature in the atmosphere varies with latitude, longitude, and altitude above the earth's surface, as well as with season and time of day (Smith, 2003). Therefore, the temperature dependence of the uptake coefficients of nitrogen dioxide on mineral dust was further investigated over the temperature range of 258–313 K, which covers the range of observed global temperatures, and can represent the common effects of temperature on these reactions. The potential of atmospheric production of HONO during these heterogeneous reactions was also investigated. The present studies provide useful information to understand the temperature dependent mechanism of the uptake and reaction processes of nitrogen dioxide on mineral dust, which is a critical factor in evaluating mineral dust environmental and climate impacts.

1. Experimental section

1.1. Reactants

The samples used in our experiments were purchased from the Chinese Standard Substance Center (the Chinese Standard Substance Center, Beijing, China). In the Standard Substance Center, Inner Mongolia desert dust and Xinjiang sierozem were collected from Inner Mongolia Wulate and Xinjiang Shihezi, respectively. The dust samples were dried first and debris was removed by sieves (0.25 mm). Then the samples were heated to 120 °C for 24 hr, crushed by a jet mill to about 20 μm, and mixed by a ball grinding mill for 48 hr. The chemical compositions of the samples are listed in Table S1. Related information can be obtained from Reference Materials Information Center of China. In our previous work, we have used the X-ray diffraction method to measure and analyze the compositions of these two mineral dusts. The major peaks were indexed to determine the mineral phases present, which showed that the main fractions were quartz and feldspar (Zhou et al., 2014). The surface areas of these powders were measured with a Quantachrome Autosob-1-C BET apparatus (autosorb-iQ, Quantachrome Instruments, USA) using multipoint Brunauer–Emmett–Teller (BET) analysis. The BET areas were determined to be 5.06 m^2/g for Inner Mongolia desert dust, and 20.98 m^2/g for Xinjiang sierozem.

Gaseous nitrogen dioxide (99.9%) purchased (Beijing Huayuan Gas Chemical industry Co., Ltd., Beijing, China) was used directly without any purification.

1.2. Knudsen cell experiments

A Knudsen cell reactor coupled with a quadrupole mass spectrometer was used to measure the uptake coefficient of nitrogen dioxide on the Inner Mongolia desert dust and Xinjiang sierozem (Chinese Standard Substance Center). This experimental apparatus has been described in detail elsewhere (Wang et al., 2011; Zhou et al., 2012).

Briefly, the Knudsen cell reactor (volume of 461 cm^3), with four isolated sample compartments and a small escape aperture, links to an electron impact ion source (EI) quadrupole mass spectrometer (HAL 3F 501, Hiden Analytical Ltd, Warrington, UK). The geometric area of the sample holder (As) was 5.3 cm^2. The effective area of the escape aperture was measured in each independent experiment according to the attenuation of the N_2 signal from one steady state to another (Li et al., 2002). It was about 0.173 cm^2 in our experiments. NO_2 was monitored by the m/z = 46 channel. The powdered samples were prepared in Teflon-coated metal sample holders, by heating a hydrosol of the powder until a dry coating of the sample remained on the bottom surface of the holder. In the Knudsen cell experiments, NO_2 gas was introduced through a leak valve to the desired pressure as measured with a wide range gauge (WRG-S-NW25, Edwards, UK). For the total uptake measurements, it was necessary to calibrate the flow out of the cell in terms of molecules per second. This was accomplished using the effective area of the escape aperture and the conversion of pressure to flux using the kinetic theory of gases. This gave the number of molecules per second escaping the cell as a function of pressure. Multiplying this value by the experimentally determined absolute pressure *versus* the quadrupole mass spectrometer (QMS) intensity data yields a conversion factor through which the NO_2 mass spectrometer signal is converted to molecular flow through the cell. Relative mass spectral sensitivities for NO_2 were determined from calibration with the pure gases. These sensitivity factors were then used in conjunction with the daily NO_2 calibration to convert the mass spectrometer signal to molecular concentration for NO_2.

When a sample was exposed to nitrogen dioxide, the signal of nitrogen dioxide molecular ion monitored at m/z = 46 dropped below its original value suddenly. An observed uptake coefficient (γ_{obs}) can be derived from the Knudsen cell Eq. (1):

$$\gamma_{obs} = \frac{A_h}{A_s}\left(\frac{I_0 - I}{I}\right) \quad (1)$$

where A_h is the effective area of the escape hole (cm^2, A_h = 0.1713 cm^2 in this study), A_s is the geometric area of the sample holder (cm^2, A_s = 5.3 cm^2 in this study), and I_0 and I

are the QMS intensities detected when sample holder is covered and exposed (dimensionless), respectively. The values obtained from this equation are the initial uptake coefficients, $\gamma_{init,obs}$ (dimensionless). In view of the reaction conditions in the Knudsen cell, which is at low pressure, data presented in our experiments can only represent the uptake process in dry conditions. It is important to view the data as representing the lower limit of the initial uptake coefficients.

In order to control temperature within the Knudsen chamber in the range from 258 to 313 K, the entire external surface of the chamber containing the samples was either heated or cooled by a circulator. For the sake of establishing an equilibrium temperature and avoiding temperature differences, the system was allowed to equilibrate after reaching a desired temperature.

1.3. Smog chamber experiments

The smog chamber used in this study is similar to the chamber reported in previous publications (Gai et al., 2011). The experimental setup consisted of a 360 L Teflon bag located in a steel box, so the experiments were carried out in dark conditions. The reactor and the analytical instruments were linked *via* Teflon tubes. The reactor was purged with purified zero-air. The pure air generator (Model 737, AADCO Instruments Inc., Cleves, Ohio, USA) was used to purify the ambient air, and then the pure air was used in the experiments. The pure air had a maximum flow rate of 250 L/min, with <0.5 ppb NO, NO_2, O_3, NH_3 and non-methane hydrocarbon (NMHC), and no detectable particles. The pure air was extremely dry, with relative humidity (RH) < 1%, so all the experiments of this work were considered to take place under dry conditions. The wall effect experiments of NO_2 and HONO were performed first. The reaction rate of NO_2 with the Teflon bag was 4.05×10^{-5} min^{-1}, and the influence of the NO_2 reaction with the Teflon bag was so small that it could be neglected. In the wall loss experiments of HONO, the gaseous HONO was generated by the reaction between $NaNO_2$ and H_2SO_4 solution in a glass washing bottle, and then the gaseous HONO was blown into the smog chamber by pure air. The HONO reaction rate with the Teflon bag was constant at about 7.18×10^{-4} min^{-1}. During the experiments, a certain concentration of NO_2 was introduced into the chamber and kept stable, and then the dust samples were rapidly introduced into the chamber through a pressurized sample line. A nozzle and sufficient pressure in the flow path ensured efficient dispersal of the samples, and the mixing time of the chamber contents was less than 30 sec. The accurate concentration of NO_2 was monitored by a NO_2 analyzer (Model 450i, Thermo Electron Corporation, USA), and its flow rate and precision were 0.7 L/min and 1 ppb, respectively. The HONO concentration was monitored by a home-made long path absorption photometer, an instrument with 1 L/min flow rate and 20 ppt precision. The instrument has a detection limit of 9×10^{-12} mol/mol and an accuracy of 10% at 5 min response time, with good linearity. After each experiment, we would turn the bag inside out and use deionized water and gauze to clean the bag. After cleaning, the wall loss rate of NO_2 would be measured again to make sure the surface of the bag was suitable for the experiments. Commonly, after about two or three experiments, we changed the bag used in the smog chamber to a new one.

2. Results and discussion

2.1. Knudsen cell experimental results

Fig. 1 shows a typical QMS signal response of mineral dusts exposed to nitrogen dioxide. The mass spectral intensity of nitrogen dioxide (m/z = 46) decreased immediately when the sample holder was opened, then the signal intensity recovered gradually to its original steady state value.

The uptake coefficients of nitrogen dioxide depend on the sample mass, and are related to the number of particle layers and total surface area. The uptake coefficient γ_{obs} is determined using the geometric surface area of the sample as a function of sample mass, as Eq. (1) is derived by assuming that the total number of the gas–surface collisions is only those occurring on the top layer. The observed mass dependence involves the diffusion of the reactant gas to underlying layers, resulting in an increase in the number of collisions with the total surface area. In this situation the entire BET area of the sample contributes to the observed uptake coefficient. As can be seen from Fig. 2, the observed uptake values are dependent on the mass of the samples. Therefore, a modification was made to the standard Knudsen cell equation in which the geometric area of the sample holder is replaced by the BET area of the sample (Underwood et al., 2000, 2001b). The plot in Fig. 2 shows the region where γ_{obs} is linearly dependent on the mass of the samples. From the plot, a mass independent uptake coefficient can be derived as

$$\gamma_{BET} = \frac{A_h}{A_{BET}}\left(\frac{I_0 - I}{I}\right) = \gamma_{obs} \times \frac{A_s}{A_{BET}} \quad (2)$$

where A_{BET} is the surface area of the sample, taken as the BET area (m^2), which is equal to the specific BET area of the powder (m^2/g) multiplied by the sample mass (g) (Underwood et al., 2001a). The results derived from each experiment were in this linear regime and summarized in Table 1.

The influence of the nitrogen dioxide concentration to the uptake coefficient was also taken into account over the range from 3.7×10^{11} to 1.2×10^{12} molecules/cm^3. On varying the initial concentration of nitrogen dioxide, there was no distinct dependence of initial uptake coefficient in this concentration range. After a long exposure time, the uptake of nitrogen dioxide on mineral dust surface showed relative saturation, such that the nitrogen dioxide signal recovered to a steady state. Besides the NO_2 (m/z = 46) channel, other ion fragments, including NO (m/z = 30), N_2O (m/z = 44) and HONO (m/z = 47) were also monitored during the uptake experiment. However, the strength of NO, N_2O or HONO signals was not affected notably by the NO_2 concentrations. According to the results obtained from experimental measurements, the heterogeneous uptake on mineral dust surface was assumed to mainly take place through physical adsorption.

There have been a number of studies concerning the uptake of NO_2 on different surfaces or materials. Very often substances that are components of crustal material are used, such as Al_2O_3, Fe_2O_3, MgO, CaO and SiO_2 (Angelini et al., 2007;

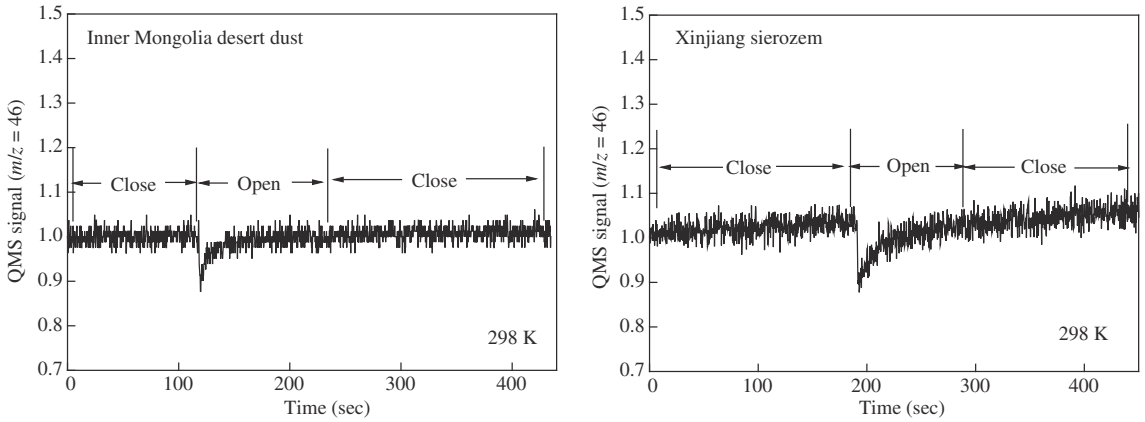

Fig. 1 – Representative Knudsen cell data for the heterogeneous uptake of NO_2 on Inner Mongolia desert dust and Xinjiang sierozem at 298 K. QMS: quadrupole mass spectrometer.

Baltrusaitis et al., 2007; Goodman et al., 1998; Grassian, 2001; Joel Gustafsson et al., 2006; Li et al., 2010; Liu et al., 2012; Miller and Grassian, 1998; Ndour et al., 2008; Szanyi et al., 2007; Underwood et al., 1999; Wu et al., 2013; Zhang et al., 2012). Furthermore, natural dust samples were also studied (Guan et al., 2014; Ndour et al., 2009; Ullerstam et al., 2003; Underwood et al., 2001b). The uptake coefficients of NO_2 on mineral aerosols are summarized in Table 2. One such study investigated the uptake of NO_2 and reported uptake coefficients of the order of 10^{-6} on China Loess and Saharan sand (Underwood et al., 2001b). Wang et al. (2012) investigated the heterogeneous reactions of NO_2 on soils collected from Dalian and Changsha over the relative humidity (RH) range of 5%–80% and temperature range of 278–328 K using a horizontal coated-wall flow tube; they reported initial uptake coefficients of the order of 10^{-7} at 297 K and RH < 5%. Consistent with previous studies, the uptake coefficients of Inner Mongolia desert dust and Xinjiang sierozem were the same order of magnitude as those for China Loess and Saharan sand; whereas, the differences in uptake coefficients from this work compared to coefficients found in the literature are likely due to the different chemical compositions and measurement conditions. It is expected that natural mineral samples with different compositions and characteristics will have different surface sites, for example quartz is the main composition in these two Chinese mineral dust samples, and the surface chemistry of SiO_2 is distinctly different from the other oxides. As shown in a previous work, the uptake coefficient for NO_2 was too low to be measured (Underwood et al., 2001b), and adsorbed water was needed if NO_2 was to react to any appreciable extent on SiO_2. In our experiments, the content of SiO_2 in the dust of Inner Mongolia desert was higher than in the dust of the Xinjiang arid region. Many studies have shown that the reactive activity of SiO_2 is lower than other oxides, and it was suggested that there would be a negative correlation between uptake coefficient and SiO_2 content. Therefore, the observed uptake coefficient of NO_2 on Xinjiang sierozem is higher than on the dust of the Inner Mongolia desert region. However, the BET area of Xinjiang sierozem is about four times larger than that of the Inner Mongolia desert dust, so that the uptake coefficients calculated using the BET areas become

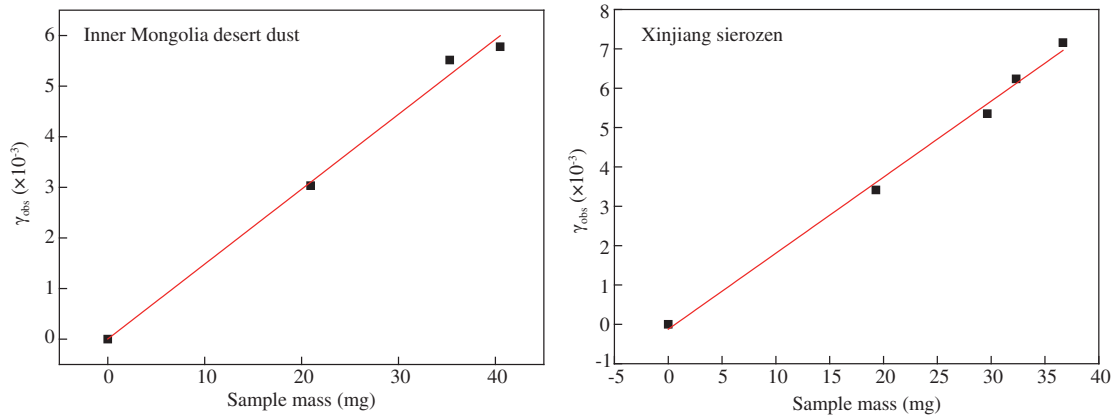

Fig. 2 – Uptake coefficient (γ_{obs}) for NO_2 on Inner Mongolia desert dust and Xinjiang sierozem calculated using the geometric surface area as the effective surface area as a function of sample mass.

Table 1 – Summary of the uptake coefficients ($\gamma_{BET,ini}$) of NO_2 on mineral dust at different temperatures.

Temperature (K)	$\gamma_{BET,int}$ ($\times 10^{-5}$) (Inner Mongolia desert dust)	$\gamma_{BET,int}$ ($\times 10^{-6}$) (Xinjiang sierozem)
258	–	4.88 ± 0.98
265	1.23 ± 0.23	–
285	1.32 ± 0.26	4.66 ± 0.93
298	1.32 ± 0.26	4.87 ± 0.97
313	1.15 ± 0.23	4.75 ± 0.95

Each value of $\gamma_{BET,ini}$ is the average of at least three measurements, and the error corresponds to one standard deviation (σ).

smaller. Thus in addition to the content of the dust, the uptake coefficient is also related to the structure of the dust.

2.2. Effect of temperature on heterogeneous reaction of NO_2 on mineral dust

The temperature dependence of the uptake coefficients of heterogeneous reactions on these mineral dust samples was further investigated over the temperature range of 258–313 K. As shown in Table 1, the initial uptake coefficients of Inner Mongolia desert dust are in the range of (1.15–1.32) × 10^{-5}, and those of Xinjiang sierozem are in the range of (4.66–4.88) × 10^{-6}. It is obvious that the initial uptake coefficients of nitrogen dioxide on the mineral dust did not change with the increase of temperature. In contrast to the findings in the current study, the rate of NO_2 conversion on γ-Al_2O_3 increased with decreasing temperature (Wu et al., 2013). This different phenomenon observed for the dependence of the initial uptake coefficients on temperature may be due to the different substances studied.

Comparing the experimental data of nitrogen dioxide uptake on different mineral dusts in our experiments, the results showed that the uptake processes of these two Chinese mineral dust samples had similarities. Based on the low uptake of NO_2, we may assume that only surface adsorption occurred. The steady state uptake coefficients of NO_2 on mineral dust are so small that the consumption of NO_2 on mineral dusts is limited. However, in real atmospheric conditions in the presence of H_2O, O_3, H_2O_2, some organic compounds or high relative humidity, further reaction probably occurs, such as the formation of HONO (Finlayson-Pitts et al., 2003; Li et al., 2010; Ndour et al., 2008), which causes more complex processes in the atmosphere, and the relationship between these reactants still needs more investigation.

2.3. Smog chamber experimental results

The smog chamber experiments were performed to monitor the kinetics of NO_2 uptake at atmospheric pressure and room temperature in order to understand the conversion of NO_2 on mineral surfaces. It is generally accepted that conversion of NO_2 on surfaces is responsible for the formation of HONO. However, the type of surface on which the mechanism occurs is still under debate.

In our experiments, the potential of atmospheric production of HONO during these heterogeneous reactions was also investigated.

First, the NO_2 decay rate constant on the Teflon surface of the chamber was taken into account. The decay rate of NO_2 on the Teflon surface of the smog chamber was 4.05 × 10^{-5} min^{-1}. It was quite small, so the NO_2 loss caused by background decay in this work was negligible. As shown in Fig. 3, when the dust was injected, the decay of NO_2 concentration as a function of time for Inner Mongolia desert dust was also quite small. The uptake coefficients of NO_2 were difficult to obtain, but this phenomenon also illustrated that the uptake of NO_2 on mineral dust samples was reversible and limited.

At the same time, in this study a home-made long path absorption photometer was used to detect the HONO formation and decomposition processes when heterogeneous reaction of NO_2 took place on Inner Mongolia desert dust. Measurement of HONO is integral to the investigation of NO_2 uptake progresses on mineral dust.

Unavoidably, the heterogeneous reaction of NO_2 with Teflon film can also produce HONO. The plot in Fig. 4 shows the region where HONO formation is linearly dependent on the concentration of NO_2. The wall loss rate of HONO, which was about 7.18 × 10^{-4} min^{-1}, had been considered.

The concentration of NO_2 in the smog chamber was about 40 ppb, which produced about 1.4 ppb HONO, so this value was the initial HONO concentration in the chamber. A total of 200 mg Inner Mongolia desert dust was injected into the smog chamber through a glass two-way valve by a zero air flush, and the HONO formation and decomposition processes were detected. Because the initial uptake coefficient of NO_2 on mineral dust is not large enough, the heterogeneous consumption of NO_2 was not considered, and the measurements were focused on the HONO formation and decomposition as outlined in Fig. 5. From Fig. 5, the estimated loss rate of HONO was about 0.246 min^{-1}, which was much more rapid than the HONO wall loss rate. It was found that HONO not only was produced though heterogeneous reaction on mineral dust, at the same time the dust surface also acted as a good sink for gas-phase HONO, which has the potential to be a source of OH radical. Mongolia desert dust and Xinjiang sierozem showed similar phenomena. Some observed data point to the minor importance of the HONO uptake on mineral aerosol (Fe_2O_3 and Arizona test dust) compared with other known sinks of HONO in the atmosphere, which are its dry deposition and photolysis in night-time and during the day (El Zein et al., 2013), while some other researchers found that a net loss of HONO to the surface was observed in the presence of reactive substrates (VandenBoer et al., 2015). It is expected that the reactive loss of HONO on the surface of mineral dust will take place in the presence of different reactive surface sites, and further study is still needed to fully understand the heterogeneous reaction process of NO_2 on mineral dust.

3. Conclusions and atmospheric implications

At present, atmospheric modeling studies have shown that mineral aerosol has a potentially significant role in the chemistry of the troposphere, by interacting with trace gases such as NO_2 and SO_2. In this study, the uptake coefficients of nitrogen dioxide on two types of Chinese mineral dust were investigated using a Knudsen cell reactor. The uptake coefficients of NO_2 on these two mineral dusts are (1.32 ± 0.26) × 10^{-5} and (4.87 ± 0.97) × 10^{-6} for

Table 2 – Summary of the uptake coefficients (γ) of NO_2 on mineral aerosols measured under different experimental conditions.

Sample	NO_2 concentration	Method	Temperature (K)	Relative humidity	γ	Reference
α-Al_2O_3	53 ppb	Knudsen cell	298		$\gamma_{0BET} = 9.1 \times 10^{-6}$	Underwood et al. (2001b)
	10.9–218.7 ppm	DRIFTS	298		$\gamma_{0BET} = (0.99 \pm 0.48) \times 10^{-9}$	Guan et al. (2014)
Illuminated γ-Al_2O_3	54.7 ppm	DRIFTS	298		$\gamma_{0BET} = (1.20–3.33) \times 10^{-9}$	Guan et al. (2014)
γ-Al_2O_3	100 ppb–10 ppm	Knudsen cell	298		$\gamma_0 = 2 \times 10^{-8}$	Underwood et al. (1999)
	500 ppb	DRIFTS	299		$\gamma_{ss,BET} = 1.3 \times 10^{-9}$	Börensen et al. (2000)
	35 ppm	DRIFTS	299		$\gamma_{ss,BET} = 2.6 \times 10^{-8}$	Börensen et al. (2000)
	53 ppb	Knudsen cell	298		$\gamma_{0,BET} = 2.0 \times 10^{-8}$	Underwood et al. (2001b)
		DRIFTS	250–318		$\gamma_{0,BET} = 8.17 \times 10^{-10}$–$2.58 \times 10^{-10}$	Wu et al. (2013)
α-Fe_2O_3	100 ppb–10 ppm	Knudsen cell	298		$\gamma_0 = 7 \times 10^{-7}$	Underwood et al. (1999)
	53 ppb	Knudsen cell	298		$\gamma_{0,BET} = 7.7 \times 10^{-6}$	Underwood et al. (2001b)
γ-Fe_2O_3	53 ppb	Knudsen cell	298		$\gamma_{0,BET} = 4.0 \times 10^{-6}$	Underwood et al. (2001b)
TiO_2	100 ppb–10 ppm	Knudsen cell	298		$\gamma_0 = 1 \times 10^{-7}$	Underwood et al. (1999)
	53 ppb	Knudsen cell	298		$\gamma_{0.BET} = 1.3 \times 10^{-7}$	Underwood et al. (2001b)
Illuminated TiO_2	1 ppm	AFT	298	15%	$\gamma = 9.6 \times 10^{-4}$	Joel Gustafsson et al. (2006)
Illuminated TiO_2	1 ppm	AFT	298	80%	$\gamma = 1.2 \times 10^{-4}$	Joel Gustafsson et al. (2006)
TiO_2/SiO_2		CWFT/LOPAP	295		$\gamma_{ss,BET} = 1 \times 10^{-9}$	Ndour et al. (2008)
Illuminated TiO_2/SiO_2		CWFT/LOPAP	295		$\gamma_{ss,BET} = 1 \times 10^{-6}$	Ndour et al. (2008)
MgO	53 ppb	Knudsen cell	298		$\gamma_{0,BET} = 1.2 \times 10^{-5}$	Underwood et al. (2001b)
CaO	53 ppb	Knudsen cell	298		$\gamma_{0,BET} = 2.2 \times 10^{-5}$	Underwood et al. (2001b)
$CaCO_3$		DRIFTS	296		$\gamma_{0,BET} = 4.3 \times 10^{-9}$	Li et al. (2010)
		DRIFTS	296	60%–71%	$\gamma_{0,BET} = 2.5 \times 10^{-9}$	Li et al. (2010)
Kaolinite	2.3 ppm	DRIFTS	298		$\gamma_{ss,BET} = 8.1 \times 10^{-8}$	Angelini et al. (2007)
	36 ppm	DRIFTS	298		$\gamma_{ss,BET} = 2.3 \times 10^{-8}$	Angelini et al. (2007)
Pyrophyllite	120 ppm	DRIFTS	298		$\gamma_{ss,BET} = 7 \times 10^{-9}$	Angelini et al. (2007)
Arizona test dust		CWFT/LOPAP	295		$\gamma_{ss,BET} = 1 \times 10^{-6}$	Ndour et al. (2008)
Na-montmorillonite	3.7–10.2 ppm	DRIFTS	298		$\gamma_{ss,BET} = 1.14 \times 10^{-8}$	Zhang et al. (2012)
Ca-montmorillonite	3.7–10.2 ppm	DRIFTS	298		$\gamma_{ss,BET} = 0.75 \times 10^{-8}$	Zhang et al. (2012)
China Loess	53 ppb	Knudsen cell	298		$\gamma_{0,BET} = 2.1 \times 10^{-6}$	Underwood et al. (2001b)
Sahara sand	53 ppb	Knudsen cell	298		$\gamma_{0,BET} = 1.2 \times 10^{-6}$	Underwood et al. (2001b)
	4.1 ppm	Knudsen cell/ DRIFTS	298		$\gamma_{0,BET} = 6.2 \times 10^{-7}$	Ullerstam et al. (2003)
		CWFT	295	25%	$\gamma_{ss,BET} = 8.9 \times 10^{-9}$	Ndour et al. (2009)
Dalian soils	50–500 ppb	CWFT	278–328	5%–80%	$\gamma_{0,BET} = 4.2 \times 10^{-8}$–$7.0 \times 10^{-8}$	Wang et al. (2012)
Changsha soils	50–500 ppb	CWFT	278–328	5%–80%	$\gamma_{0,BET} = 5.53 \times 10^{-8}$–$9.14 \times 10^{-8}$	Wang et al. (2012)
Inner Mongolia desert dust	15–50 ppb	Knudsen cell	258–313		$\gamma_{0,BET} = 1.15 \times 10^{-5}$–$1.32 \times 10^{-5}$	This work
Xinjiang sierozem	15–50 ppb	Knudsen cell	258–313		$\gamma_{0,BET} = 4.66 \times 10^{-6}$–$4.88 \times 10^{-6}$	This work

DRIFTS: diffuse reflectance infrared Fourier transform spectroscopy; AFT: aerosol flow tube; CWFT/LOPAP: coated wall flow tube reactor/long path absorption photometer.
$\gamma_{0,BET}$: initial BET uptake coefficient; $\gamma_{ss,BET}$: steady state uptake coefficient; γ_0: initial uptake coefficient.

Inner Mongolia desert dust and Xinjiang sierozem respectively at 298 K and dry conditions. In agreement with a previous study on NO_2 uptake on China loess, uptake coefficients on Chinese mineral dust uptake are mainly on the order of 10^{-6}. Moreover, it is important to view the data presented in our experiments as lower limits of the initial uptake coefficients. In addition, the temperature had little effect on the initial uptake coefficients for these two kinds of Chinese mineral dust.

In contrast to the previously used methods, the Knudsen cell reactor enables the detection of low concentrations, so this process can now be studied under atmospherically relevant concentrations. The rate of removal of nitrogen dioxide by uptake onto mineral dust can be estimated using a simple model. The lifetime of nitrogen dioxide due to uptake onto Inner Mongolia desert dust and Xinjiang sierozem can be estimated by:

$$\tau = \frac{4}{\gamma \bar{c} A} \quad (3)$$

where A (cm^2/cm^3) is the dust surface area density, $\bar{c}$ is the mean molecular speed, and γ is the uptake coefficient. Because BET

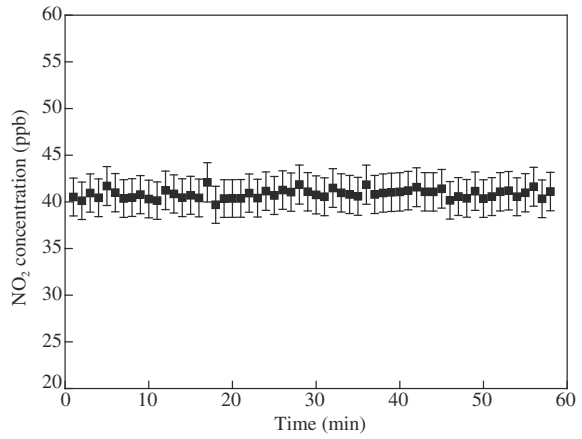

Fig. 3 – Profile of NO_2 concentration after introduction of Inner Mongolia desert dust (200 mg) into the chamber.

areas are applicable for calculating the uptake coefficients, here we use them as dust surface areas. If we assume a conservatively low dust loading of 5 μg/m^3 to a high dust loading of 600 μg/m^3 (Aymoz et al., 2004; Guo et al., 2013; Li et al., 2012), we obtain $A \approx 2.5 \times 10^{-5}$ to 3×10^{-3} m^2/m^3 for Inner Mongolia desert dust and $A \approx 1.05 \times 10^{-4}$ to 1.26×10^{-2} m^2/m^3 for Xinjiang sierozem. Our measured uptake coefficients are about $(1.32 \pm 0.26) \times 10^{-5}$ and $(4.87 \pm 0.97) \times 10^{-6}$ for Inner Mongolia desert dust and Xinjiang sierozem, respectively, which lead to the corresponding atmospheric lifetimes with respect to processing by Inner Mongolia desert dust and Xinjiang sierozem of 3.2 to 381.2, and 2.1 to 246.0 days, respectively. The uptake coefficients calculated based on the BET surface area of the dust samples represent a lower limit. As for the Arizona test dust, the BET surface area is about 4 times larger compared with the geometric area (Wagner et al., 2009), which may cause γ_{BET} to be a factor of 4 smaller than that calculated based on the geometric surface area. This gap should also be taken into account in the box model study, which would cause an underestimation of NO_2 transformation. When sand storms occur, the surface mass aerosol concentrations may reach a peak of 3000 μg/m^3 (Li et al., 2012). In that case, the interaction between mineral aerosol and nitrogen

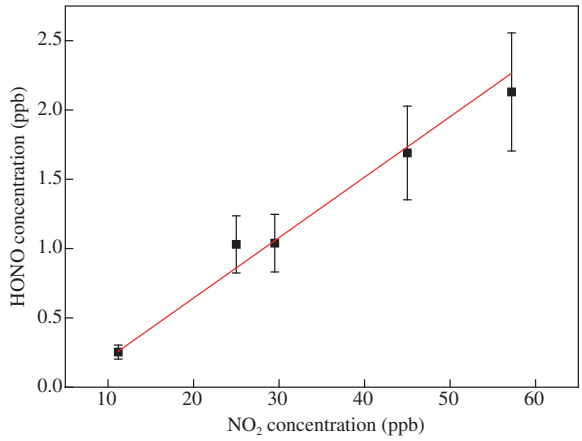

Fig. 4 – Dependence of the concentration of HONO formation on Teflon film surface as a function of the NO_2 gas phase concentration.

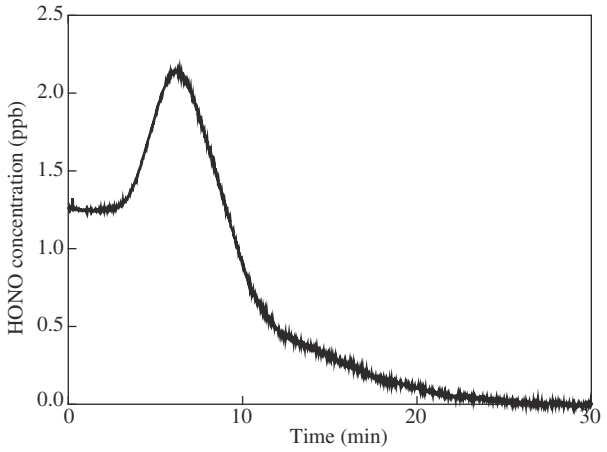

Fig. 5 – Profile of HONO concentration after Inner Mongolia desert dust (200 mg) was introduced into 360 L chamber with NO_2 (about 40 ppb).

dioxide can dramatically influence the concentration of nitrogen dioxide in the atmosphere, and the dust surface can also be a night-time sink of nitrous acid at the same time.

In conclusion, it should be noted that although the NO_2 reaction with mineral dust has a limited atmospheric impact, the kinetic and especially product data from the present study has the potential to be very useful and should be accounted for in laboratory studies of potential heterogeneous sources and consumption of nitrous acid.

Acknowledgments

This project was supported by the National Basic Research Program (973) of Ministry of Science and Technology of China (No. 2011CB403401), the National Natural Science Foundation of China (Nos. 21190052, 41173112, and 41475114), and the Strategic Priority Research Program (B) of the Chinese Academy of Sciences (No. XDB05010400).

Appendix A. Supplementary data

Supplementary data to this article can be found online at http://dx.doi.org/10.1016/j.jes.2015.05.017.

REFERENCES

Al-Abadleh, H.A., Krueger, B.J., Ross, J.L., Grassian, V.H., 2003. Phase transitions in calcium nitrate thin films. Chem. Commun. 22, 2796–2797.

Angelini, M.M., Garrard, R.J., Rosen, S.J., Hinrichs, R.Z., 2007. Heterogeneous reactions of gaseous HNO_3 and NO_2 on the clay minerals kaolinite and pyrophyllite. J. Phys. Chem. A111 (17), 3326–3335.

Aymoz, G., Jaffrezo, J.L., Jacob, V., Colomb, A., George, C., 2004. Evolution of organic and inorganic components of aerosol during a Saharan dust episode observed in the French Alps. Atmos. Chem. Phys. 4 (11-12), 2499–2512.

Baltrusaitis, J., Schuttlefield, J., Jensen, J.H., Grassian, V.H., 2007. FTIR spectroscopy combined with quantum chemical calculations to investigate adsorbed nitrate on aluminium oxide surfaces in the presence and absence of co-adsorbed water. Phys. Chem. Chem. Phys. 9 (36), 4970–4980.

Börensen, C., Kirchner, U., Scheer, V., Vogt, R., Zellner, R., 2000. Mechanism and kinetics of the reactions of NO_2 or HNO_3 with alumina as a mineral dust model compound. J. Phys. Chem. A 104 (21), 5036–5045.

Carmichael, G.R., Hong, M.S., Ueda, H., Chen, L.L., Murano, K., Park, J.K., et al., 1997. Aerosol composition at Cheju Island, Korea. J. Geophys. Res. Atmos. 102 (D5), 6047–6061.

Cwiertny, D.M., Young, M.A., Grassian, V.H., 2008. Chemistry and photochemistry of mineral dust aerosol. Annu. Rev. Phys. Chem. 59 (1), 27–51.

Dentener, F.J., Carmichael, G.R., Zhang, Y., Lelieveld, J., Crutzen, P.J., 1996. Role of mineral aerosol as a reactive surface in the global troposphere. J. Geophys. Res. Atmos. 101 (D17), 22869–22889.

El Zein, A., Romanias, M.N., Bedjanian, Y., 2013. Kinetics and products of heterogeneous reaction of HONO with Fe_2O_3 and Arizona test dust. Environ. Sci. Technol. 47 (12), 6325–6331.

Febo, A., Perrino, C., Allegrini, I., 1996. Measurement of nitrous acid in Milan, Italy, by DOAS and diffusion denuders. Atmos. Environ. 30 (21), 3599–3609.

Finlayson-Pitts, B.J., Wingen, L.M., Sumner, A.L., Syomin, D., Ramazan, K.A., 2003. The heterogeneous hydrolysis of NO_2 in laboratory systems and in outdoor and indoor atmospheres: an integrated mechanism. Phys. Chem. Chem. Phys. 5 (2), 223–242.

Gai, Y.B., Ge, M.F., Wang, W.G., 2011. Kinetics of the gas-phase reactions of some unsaturated alcohols with Cl atoms and O_3. Atmos. Environ. 45 (1), 53–59.

Goodman, A.L., Miller, T.M., Grassian, V.H., 1998. Heterogeneous reactions of NO_2 on NaCl and Al_2O_3 particles. J. Vac. Sci. Technol. A 16 (4), 2585–2590.

Grassian, V.H., 2001. Heterogeneous uptake and reaction of nitrogen oxides and volatile organic compounds on the surface of atmospheric particles including oxides, carbonates, soot and mineral dust: implications for the chemical balance of the troposphere. Int. Rev. Phys. Chem. 20 (3), 467–548.

Guan, C., Li, X.L., Luo, Y.Q., Huang, Z., 2014. Heterogeneous reaction of NO_2 on α-Al_2O_3 in the dark and simulated sunlight. J. Phys. Chem. A 118 (34), 6999–7006.

Guo, J.P., Niu, T., Wang, F., Deng, M.J., Wang, Y.Q., 2013. Integration of multi-source measurements to monitor sand-dust storms over North China: a case study. Acta Meteor. Sin. 27 (4), 566–576.

Harrison, S.P., Kohfeld, K.E., Roelandt, C., Claquin, T., 2001. The role of dust in climate changes today, at the last glacial maximum and in the future. Earth-Sci. Rev. 54 (1-3), 43–80.

Joel Gustafsson, R., Orlov, A., Griffiths, P.T., Anthony Cox, R., Lambert, R.M., 2006. Reduction of NO_2 to nitrous acid on illuminated titanium dioxide aerosol surfaces: implications for photocatalysis and atmospheric chemistry. Chem. Commun. 37, 3936–3938.

Kleffmann, J., 2007. Daytime sources of nitrous acid (HONO) in the atmospheric boundary layer. ChemPhysChem 8 (8), 1137–1144.

Li, J.W., Han, Z.W., 2010. A modeling study of the impact of heterogeneous reactions on mineral aerosol surfaces on tropospheric chemistry over East Asia. Particuology 8 (5), 433–441.

Li, P., Al-Abadleh, H.A., Grassian, V.H., 2002. Measuring heterogeneous uptake coefficients of gases on solid particle surfaces with a Knudsen cell reactor: complications due to surface saturation and gas diffusion into underlying layers. J. Phys. Chem. A106 (7), 1210–1219.

Li, H.J., Zhu, T., Zhao, D.F., Zhang, Z.F., Chen, Z.M., 2010. Kinetics and mechanisms of heterogeneous reaction of NO_2 on $CaCO_3$ surfaces under dry and wet conditions. Atmos. Chem. Phys. 10 (2), 463–474.

Li, J., Wang, Z., Zhuang, G., Luo, G., Sun, Y., Wang, Q., 2012. Mixing of Asian mineral dust with anthropogenic pollutants over East Asia: a model case study of a super-duststorm in March 2010. Atmos. Chem. Phys. 12 (16), 7591–7607.

Lisachenko, A.A., Klimovskii, A.O., Mikhailov, R.V., Shelimov, B.N., Che, M., 2006. Mass spectrometric study of heterogeneous chemical and photochemical reactions of NOx on alumina taken as a model substance for mineral aerosol. Appl. Catal. B Environ. 67 (1-2), 127–135.

Liu, C., Ma, Q.X., Liu, Y.C., Ma, J.Z., He, H., 2012. Synergistic reaction between SO_2 and NO_2 on mineral oxides: a potential formation pathway of sulfate aerosol. Phys. Chem. Chem. Phys. 14 (5), 1668–1676.

Miller, T.M., Grassian, V.H., 1998. Heterogeneous chemistry of NO_2 on mineral oxide particles: spectroscopic evidence for oxide-coordinated and water-solvated surface nitrate. Geophys. Res. Lett. 25 (20), 3835–3838.

Ndour, M., D'Anna, B., George, C., Ka, O., Balkanski, Y., Kleffmann, J., et al., 2008. Photoenhanced uptake of NO_2 on mineral dust: laboratory experiments and model simulations. Geophys. Res. Lett. 35 (5). http://dx.doi.org/10.1029/2008GL036662.

Ndour, M., Nicolas, M., D'Anna, B., Ka, O., George, C., 2009. Photoreactivity of NO_2 on mineral dusts originating from different locations of the Sahara desert. Phys. Chem. Chem. Phys. 11 (9), 1312–1319.

Nie, W., Wang, T., Xue, L.K., Ding, A.J., Wang, X.F., Gao, X.M., et al., 2012. Asian dust storm observed at a rural mountain site in southern China: chemical evolution and heterogeneous photochemistry. Atmos. Chem. Phys. 12 (24), 11985–11995.

Ooki, A., Uematsu, M., 2005. Chemical interactions between mineral dust particles and acid gases during Asian dust events. J. Geophys. Res. Atmos. 110 (D3). http://dx.doi.org/10.1029/2004jd004737.

Prospero, J.M., 1999. Long-term measurements of the transport of African mineral dust to the southeastern United States: implications for regional air quality. J. Geophys. Res. Atmos 104 (D13), 15917–15927.

Smith, I.W.M., 2003. Laboratory studies of atmospheric reactions at low temperatures. Chem. Rev. 103 (12), 4549–4564.

Song, C.H., Carmichael, G.R., 2001. A three-dimensional modeling investigation of the evolution processes of dust and sea-salt particles in east Asia. J. Geophys. Res. Atmos 106 (D16), 18131–18154.

Sullivan, R.C., Guazzotti, S.A., Sodeman, D.A., Tang, Y., Carmichael, G.R., Prather, K.A., 2007. Mineral dust is a sink for chlorine in the marine boundary layer. Atmos. Environ. 41 (34), 7166–7179.

Szanyi, J., Kwak, J.H., Chimentao, R.J., Peden, C.H.F., 2007. Effect of H_2O on the adsorption of NO_2 on γ-Al_2O_3: an in situ FTIR/MS study. J. Phys. Chem. C 111 (6), 2661–2669.

Tang, Y.H., Carmichael, G.R., Kurata, G., Uno, I., Weber, R.J., Song, C.H., et al., 2004. Impacts of dust on regional tropospheric chemistry during the ACE-Asia experiment: a model study with observations. J. Geophys. Res. Atmos. 109 (D19). http://dx.doi.org/10.1029/2003JD003806.

Ullerstam, M., Johnson, M.S., Vogt, R., Ljungström, E., 2003. DRIFTS and Knudsen cell study of the heterogeneous reactivity of SO_2 and NO_2 on mineral dust. Atmos. Chem. Phys. 3 (6), 2043–2051.

Underwood, G.M., Miller, T.M., Grassian, V.H., 1999. Transmission FT-IR and Knudsen cell study of the heterogeneous reactivity of gaseous nitrogen dioxide on mineral oxide particles. J. Phys. Chem. A 103 (31), 6184–6190.

Underwood, G.M., Li, P., Usher, C.R., Grassian, V.H., 2000. Determining accurate kinetic parameters of potentially important heterogeneous atmospheric reactions on solid particle surfaces with a Knudsen cell reactor. J. Phys. Chem. A 104 (4), 819–829.

Underwood, G.M., Li, P., Al-Abadleh, H., Grassian, V.H., 2001a. A Knudsen cell study of the heterogeneous reactivity of nitric acid on oxide and mineral dust particles. J. Phys. Chem. A 105 (27), 6609–6620.

Underwood, G.M., Song, C.H., Phadnis, M., Carmichael, G.R., Grassian, V.H., 2001b. Heterogeneous reactions of NO_2 and HNO_3 on oxides and mineral dust: a combined laboratory and modeling study. J. Geophys. Res. Atmos. 106 (D16), 18055–18066.

Usher, C.R., Michel, A.E., Grassian, V.H., 2003. Reactions on mineral dust. Chem. Rev. 103 (12), 4883–4939.

VandenBoer, T.C., Young, C.J., Talukdar, R.K., Markovic, M.Z., Brown, S.S., Roberts, J.M., et al., 2015. Nocturnal loss and daytime source of nitrous acid through reactive uptake and displacement. Nat. Geosci. 8, 55–60. http://dx.doi.org/10.1038/ngeo2298.

Wagner, C., Hanisch, F., Holmes, N., de Coninck, H., Schuster, G., Crowley, J.N., 2008. The interaction of N_2O_5 with mineral dust: aerosol flow tube and Knudsen reactor studies. Atmos. Chem. Phys. 8 (1), 91–109.

Wagner, C., Schuster, G., Crowley, J.N., 2009. An aerosol flow tube study of the interaction of N_2O_5 with calcite, Arizona dust and quartz. Atmos. Environ. 43 (32), 5001–5008.

Wang, S., Ackermann, R., Spicer, C.W., Fast, J.D., Schmeling, M., Stutz, J., 2003. Atmospheric observations of enhanced NO_2–HONO conversion on mineral dust particles. Geophys. Res. Lett. 30 (11), 1595. http://dx.doi.org/10.1029/2003GL017014.

Wang, W.G., Ge, M.F., Sun, Q., 2011. Heterogeneous uptake of hydrogen peroxide on mineral oxides. Chin. J. Chem. Phys. 24 (5), 515–520.

Wang, L., Wang, W.G., Ge, M.F., 2012. Heterogeneous uptake of NO_2 on soils under variable temperature and relative humidity conditions. J. Environ. Sci. 24 (10), 1759–1766.

Wu, L.Y., Tong, S.R., Ge, M.F., 2013. Heterogeneous reaction of NO_2 on Al_2O_3: the effect of temperature on the nitrite and nitrate formation. J. Phys. Chem. A117 (23), 4937–4944.

Zamaraev, K.I., Khramov, M.I., Parmon, V.N., 1994. Possible impact of heterogeneous photocatalysis on the global chemistry of the earth's atmosphere. Catal. Rev. 36 (4), 617–644.

Zhang, Z.F., Shang, J., Zhu, T., Li, H.J., Zhao, D.F., Liu, Y.J., et al., 2012. Heterogeneous reaction of NO_2 on the surface of montmorillonite particles. J. Environ. Sci. 24 (10), 1753–1758.

Zhou, L., Wang, W.G., Ge, M.F., 2012. Temperature dependence of heterogeneous uptake of hydrogen peroxide on silicon dioxide and calcium carbonate. J. Phys. Chem. A 116 (30), 7959–7964.

Zhou, L., Wang, W.G., Gai, Y.B., Ge, M.F., 2014. Knudsen cell and smog chamber study of the heterogeneous uptake of sulfur dioxide on Chinese mineral dust. J. Environ. Sci. 26 (12), 2423–2433.